Adsorption and Surface Reaction of NO2 on a Stepped Au(997) Surface: Enhanced Reactivity of Low-Coordinated Au Atoms

ARTICLE *in* THE JOURNAL OF PHYSICAL CHEMISTRY C · JANUARY 2012

Impact Factor: 4.77 · DOI: 10.1021/jp210028y

7 AUTHORS, INCLUDING:

Zongfang Wu
Fritz Haber Institute of the Max Planck Society
19 PUBLICATIONS **176** CITATIONS
SEE PROFILE

Yulin Zhang
University of Science and Technology of China
8 PUBLICATIONS **108** CITATIONS
SEE PROFILE

Lingshun Xu
University of Science and Technology of China
18 PUBLICATIONS **205** CITATIONS
SEE PROFILE

Weixin Huang
University of Science and Technology of China
106 PUBLICATIONS **1,958** CITATIONS
SEE PROFILE

THE JOURNAL OF PHYSICAL CHEMISTRY C

Article

pubs.acs.org/JPCC

Adsorption and Surface Reaction of NO_2 on a Stepped Au(997) Surface: Enhanced Reactivity of Low-Coordinated Au Atoms

Zongfang Wu,[†,‡,§] Yunsheng Ma,[§] Yulin Zhang,[†,‡,§] Lingshun Xu,[†,‡,§] Bohao Chen,[†,‡,§] Qing Yuan,[†,‡,§] and Weixin Huang*[,†,‡,§]

[†]Hefei National Laboratory for Physical Sciences at the Microscale, [‡]CAS Key Laboratory of Materials for Energy Conversion, and [§]Department of Chemical Physics, University of Science and Technology of China, Hefei 230026, China

ABSTRACT: The adsorption and surface reaction of NO_2 on a stepped Au(997) surface were investigated by temperature-programmed desorption, X-ray photoelectron spectroscopy, and ultraviolet photoelectron spectroscopy. At low NO_2 exposures, NO_2 chemisorbs molecularly and reversibly on the Au(997) surface at 130 K, but low-coordinated Au atoms on the (111) step sites exhibit enhanced reactivity. NO_2(a) chemisorbed on the (111) step sites is thermally more stable than that chemisorbed on the (111) terrace sites. At large NO_2 exposures, an amorphous physisorbed N_2O_4 multilayer forms at 130 K. Subsequent heating causes the isomerization of the physisorbed N_2O_4 multilayer (O_2N-NO_2) to nitrite–N_2O_4 ($ONO-NO_2$) and the subsequent transformation of nitrite–N_2O_4 into nitrosonium nitrate ($NO^+NO_3^-$) that further decomposes into NO(g) and NO_2(g) at elevated temperatures, forming O(a) on the surface. These surface reactions could be utilized to prepare oxygen adatoms on inert Au surfaces under ultrahigh vacuum conditions. Our results broaden the fundamental understanding of the interaction between small molecules and Au surfaces.

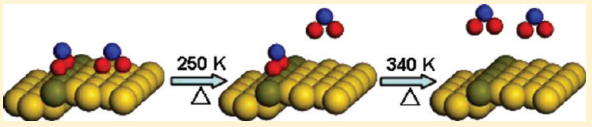

1. INTRODUCTION

The interaction between NO_2 and metal surfaces has attracted great interest in the past decades since such an interaction is important in many fields such as heterogeneous catalysis, environmental protection, and gas sensors. NO_2 exhibits a very rich chemistry on metal surfaces which largely depends on the type of the substrate, surface structure, and substrate temperature.[1−23] After adsorption, it can undergo reversible adsorption/desorption,[1−4] partial dissociation ($NO_2 \rightarrow NO + O$),[5,6,9−12,14,16,19,23] complete dissociation ($NO_2 \rightarrow N + O$),[8,17,21] or surface reaction to form surface NO_3 species.[13,15,18,22]

The interaction between NO_2 and the Au surface is now receiving much attention both fundamentally and practically. The Au surface had long been considered catalytically inert but recently has been demonstrated to be versatile in catalyzing a series of important catalytic reactions including the selective oxidation reaction with NO_2.[24] Several investigations have been previously reported on the adsorption and reaction behavior of NO_2 on Au single crystal surfaces; however, some controversies still exist, and further investigations on Au–NO_2 interactions are needed.[1,2,4,25−27] Bartram and Koel have reported that NO_2 is adsorbed molecularly and reversibly on Au(111) at 100 K.[1] After saturation of chemisorbed NO_2 (saturation coverage ∼ 0.4 ML), a N_2O_4 multilayer can be formed.[1] On the polycrystalline gold surface, temperature-programmed desorption (TPD) and high-resolution electron energy loss spectroscopy (HREELS) results showed no evidence for NO_2 dissociation on such a defect-rich surface even for large exposures of NO_2 at surface temperature up to 500 K.[25] In contrast, on the basis of thermal desorption spectroscopy (TDS) results, Sato et al. proposed that chemisorbed NO_2 is partly decomposed to NO and O(a) on Au(111), but O_2 desorption was observed at 507 K only when the adsorption–desorption cycle of chemisorbed NO_2 had been repeated a few times below 400 K to accumulate oxygen adatoms on the surface.[4] This may be due to that O(a) can easily react with NO(g) released by NO_2 decomposition on the wall of the ultrahigh vacuum (UHV) chamber,[1] to form NO_2(a) on the surface, and desorbs as NO_2(g) from the surface at higher temperatures.[28−30]

On the other hand, since the pioneered work by Haruta et al.,[31] it has been found that the size of supported gold nanoparticles strongly affects their catalytic performance. The strong size-dependent catalytic activity of Au nanocatalysts has been popularly attributed to the presence of low-coordinated and thus reactive Au atoms on small Au nanoparticles.[32] Such active Au sites can be modeled by using stepped Au single-crystal surfaces under UHV conditions, and some interesting results have been reported. It has been shown that CO adsorption energy is not only dependent on the coordination number of the Au atoms but also on the exact geometrical structure.[33] CO can not adsorb on perfect Au(111), Au(100), and Au(311) surfaces at 120 K at CO pressures up to 0.01 Torr,[34] but CO adsorption was observed on Au(310), Au(321), Au(110)-(1 × 2), and Au(332) surfaces in the temperature range of 90–100 K.[33,35,36] It was reported that NO can not adsorb on defect-free Au(111) even at temperatures of 90 K[1] but can adsorb on Au(111) with surface defects.[28] Furthermore, NO can even decompose into N_2O on Au(310) at

Received: October 19, 2011
Revised: December 3, 2011
Published: January 10, 2012

temperature as low as 80 K.[37] A recent study by DFT calculations also indicates that NO adsorption on the edge of the step sites of Au(321) is more stable than that on the planar (111) surface.[38] To our knowledge, no literature has been reported on the adsorption and surface reaction of NO_2 on stepped Au single-crystal surfaces up to now. Therefore, it is of interest to investigate the activity of low-coordinated Au atoms toward NO_2 adsorption and dissociation.

In the present study, the adsorption and surface reaction of NO_2 on a Au(997) surface were investigated by temperature-programmed desorption (TDS), X-ray photoelectron spectroscopy (XPS), and ultraviolet photoelectron spectroscopy (UPS). Low coordinated Au atoms on the (111) steps were demonstrated to exhibit enhanced reactivity toward NO_2 chemisorption, but no NO_2 decomposition was observed. Upon heating, the amorphous physisorbed N_2O_4 multilayer on the Au(997) surface could transform into a nitrosonium nitrate ($NO^+NO_3^-$) intermediate which further decomposes to NO(g) and NO_2(g), producing O(a) on the surface.

2. EXPERIMENTAL SECTION

All experiments were performed in a Leybold stainless-steel UHV chamber with a base pressure of $1-2 \times 10^{-10}$ mbar equipped with facilities for XPS, low-energy electron diffraction (LEED), and differential-pumped TDS measurements.[39] The UHV chamber has been recently updated with a new hemispherical energy analyzer (PHBIOS 100 MCD, SPECS GmbH), X-ray source (XR 50, SPECS GmbH), and UV source (UVS 10/35, SPECS GmbH). A Au(997) single crystal purchased from MaTeck was mounted on the sample holder by two Ta wires spot-welded to the back side of the sample. The sample temperature could be controlled between 130 and 1473 K and was measured by a chromel-alumel thermocouple spot-welded to the backside of the sample. Prior to the experiments, the Au sample was cleaned by repeated cycles of Ar ion sputtering and annealing until LEED gave a sharp diffraction pattern and no contaminants could be detected by XPS.

NO_2 (>99.9%, Nanjing ShangYuan Industry Factory) and NO (>99.9%, Nanjing ShangYuan Industry Factory) were used as received without any further purification; ultrapure water (resistance >18MΩ) was purified by repeated freeze−pump−thaw cycles; and all their purities were further checked by a quadrupole mass spectrometer (QMS) prior to experiments. It is noteworthy that the mass spectrum of NO_2 in our QMS gave an intensity ratio of amu 30/amu 46 to be 33. The base pressure of the chamber during the course of NO_2 exposure was controlled to be below 5×10^{-10} Torr; therefore, a line-of-sight stainless steel doser (diameter: 8 mm) positioned ~2 mm in front of the Au surface was used for relatively large NO_2 exposures. To decrease the possibility of NO_2 dissociation, the gas line was flushed by NO_2 several times before each experiment. The exposures of NO_2 reported herein were corrected with the enhancement effect of the doser (~1000).[40] All exposures were reported in Langmuir ($1\ L = 1.0 \times 10^{-6}$ Torr·s) without corrections for the gauge sensitivity.

During the TDS experiments, the Au sample was positioned ~1 mm away from the collecting tube of a differential-pumped QMS and heated to 650 K with a heating rate of 3.0 K/s. The signals with m/e = 30 (NO), 46 (NO_2), 18 (H_2O), 28 (CO and N_2), and 44 (CO_2 and N_2O) were monitored simultaneously. XPS spectra were recorded with a pass energy of 20 eV using Al Kα radiation (hν = 1486.6 eV). UPS spectra were recorded with a pass energy of 2 eV using He II radiation (hν = 40.8 eV).

3. RESULTS AND DISCUSSION

The Au(997) vicinal surface is created by cutting a Au(111) crystal at an angle of approximately 7° offset to obtain atomic height steps along the dense [1$\bar{1}$0] direction separated by (111) terraces, whose surface structure is schematically shown in Figure 1. The (997) vicinal surface of face-centered cubic

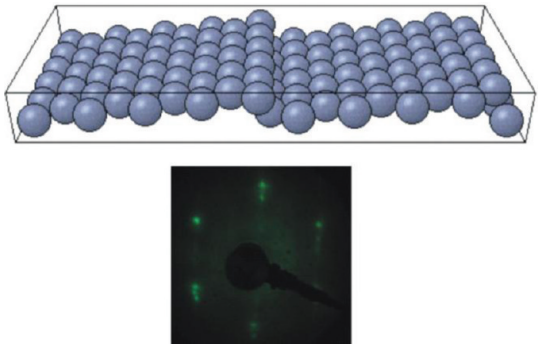

Figure 1. (Top) Schematic structural illustration and (bottom) LEED pattern of stepped Au(997) surface. E_p = 85 eV.

metals is composed of close-packed (111) terraces and a monatomic step with (111) microfacet. The coordination number of Au atoms on the monatomic step of Au(997) is 7, lower than that of Au atoms on the terrace of Au(997) (9). The LEED pattern of the clean Au(997) surface (Figure 1) is with splitting spots forming a hexagonal symmetry, similar to the LEED patterns of Pt(997) and Cu(997).[41,42]

Figures 2A and 2B show the desorption traces of NO_2 after various exposures of NO_2 on clean Au(997) at 130 K. No obvious NO_2 desorption peaks were observed for very low NO_2 exposures. A desorption peak (denoted as β) first appears at ~240 K for a NO_2 exposure of 0.02 L. It grows with the increase of NO_2 exposure and saturates at a NO_2 exposure of 0.1 L. Following 0.1 L NO_2 exposure, another desorption feature (denoted as γ_1) appears at ~164 K, which exhibits a characteristic of zero-order desorption kinetics and does not saturate with the increase of NO_2 exposure. Thus, the γ_1 peak reasonably corresponds to desorption of the N_2O_4 multilayer layer.

Figures 2C−2E display the accompanying desorption traces of NO that totally give five desorption peaks. A desorption peak (denoted as α) first appears at ~340 K at a NO_2 exposure of 0.001 L. It grows with the increase of NO_2 exposure and saturates at a NO_2 exposure of 0.005 L. Meanwhile, another peak (denoted as β) emerges at ~240 K which then saturates at a NO_2 exposure of 0.1 L. An additional three desorption peaks denoted as γ_1, γ_2, and γ_3 also appear at ~164, ~180, and ~204 K, respectively. The γ_1 peak exhibits a characteristic of zero-order desorption kinetics and does not saturate with the increase of NO_2 exposure.

By comparing desorption traces of NO_2 and NO (insets in Figures 2B and 2D), it can be deduced that the β and γ_1 desorption traces of NO arise from the fragmentation of β and γ_1 desorption traces of NO_2, respectively. The β desorption peak of NO_2 from Au(997) is similar to the desorption peak of NO_2(a) chemisorbed on Au(111);[1] therefore, it can be assigned to NO_2(a) chemisorbed on the (111) terraces of

dx.doi.org/10.1021/jp210028y | J. Phys. Chem. C 2012, 116, 3608−3617

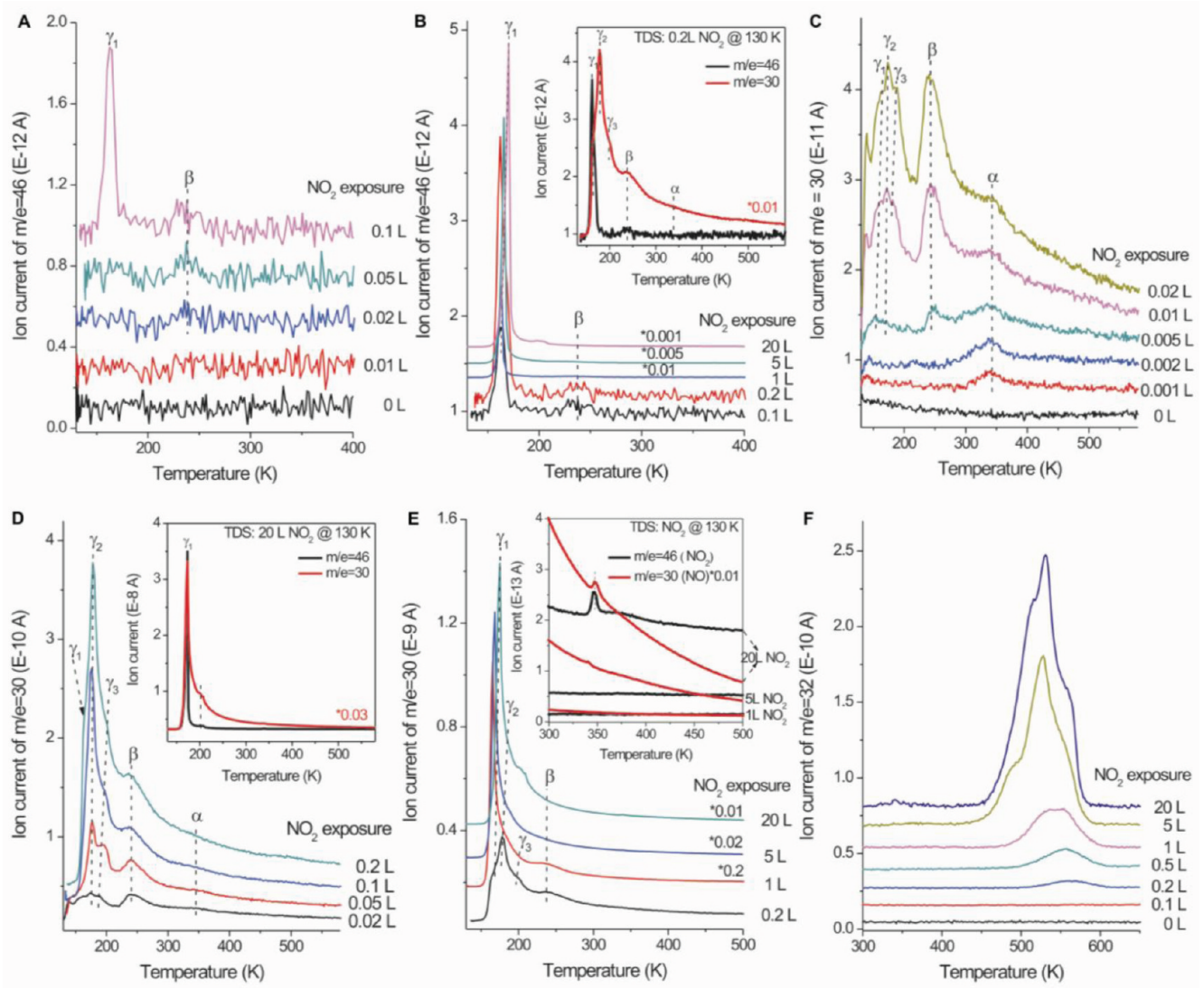

Figure 2. (A,B) NO_2 (m/e = 46), (C–E) NO (m/e = 30), and (F) O_2 (m/e = 32) TDS spectra after Au(997) was exposed to different amounts of NO_2 at 130 K.

Au(997). The α desorption peak of NO at ~340 K is not accompanied with a corresponding NO_2 desorption trace; however, it could not arise from the desorption of NO(a) from Au(997) although it was previously reported that NO(g) would more or less be introduced in the background due to the decomposition of NO_2(g) on the wall of the UHV chamber during the course of NO_2 exposure.[1] We have studied the adsorption of NO(g) on Au(997) at 130 K in which a single NO desorption peak arising from NO(a) on the (111) steps of Au(997) was observed at ~170 K after the saturating NO exposure (Figure 10). We thus assigned the α desorption peak to the desorption of NO_2(a) chemisorbed on the (111) steps of Au(997), whose absence in the NO_2 desorption spectra is due to its low intensity beyond the detection limit of our QMS. It can be seen that after an exposure of 0.01 L NO_2 the β desorption peak of NO resulting from the desorption peak of NO_2(a) on the (111) terraces of Au(997) is much stronger than the α desorption peak of NO (Figure 2C) but still fails to give a clear corresponding NO_2 desorption trace (Figure 2A); therefore, it is understandable that the desorption of NO_2(a) on the (111) steps of Au(997) only gives the α desorption peak of NO but not the corresponding peak of NO_2.

Although exhibiting stronger intensities than the saturating β desorption peak of NO, two NO desorption features at ~204 and ~180 K are not accompanied by NO_2 desorption, indicating that they can not be attributed to the fragmentation of desorbed NO_2 in the mass spectrometer; meanwhile, both desorption peaks could be clearly observed after a NO_2 exposure of 0.05 L, but no oxygen desorption signals could be detected (Figure 2F), indicating that they are not likely to result from NO_2(a) decomposition on the surface. Bartram and Koel previously reported that NO can not adsorb on Au(111), at 90 K, but chemisorbed NO_2(a) can react with NO(g) to form N_2O_3(a) on the surface that decomposes into NO_2(a) and NO(g) at ~170 K in the subsequent heating.[1] NO can also chemisorb on the (111) steps of Au(997) at 130 K, which gives a single NO desorption peak at ~170 K after the saturating NO exposure (Figure 10). Therefore, we tentatively assigned these two NO desorption peaks at ~204 and ~180 K after the exposure of NO_2 on Au(997) at 130 K to NO-involved surface species, either NO(a) chemisorbed on the step sites of Au(997) or N_2O_3(a) formed by NO_2(a) with NO(g) on Au(997). Interestingly, additional NO and NO_2 desorption peaks were clearly and reproducibly detected at ~350 K when NO_2

dx.doi.org/10.1021/jp210028y | J. Phys. Chem. C 2012, 116, 3608–3617

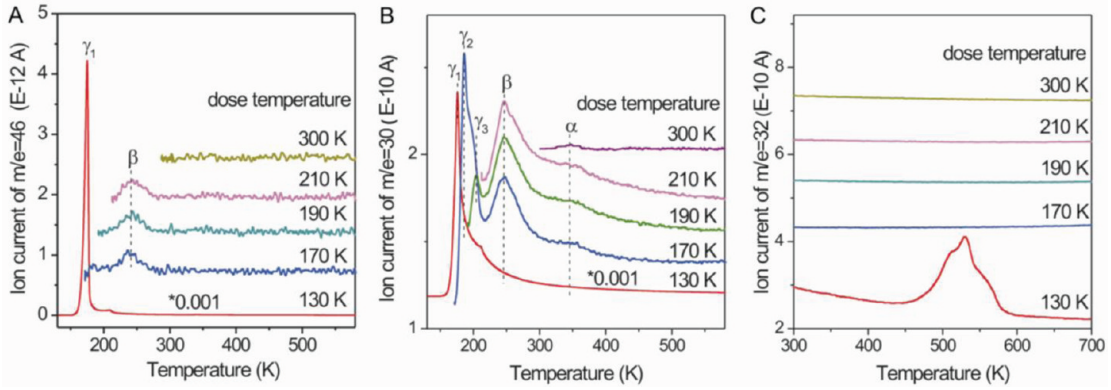

Figure 3. (A) NO_2 (m/e = 46) and (B) NO (m/e = 30) and (C) O_2 (m/e = 32) TDS spectra after Au(997) was exposed to 20 L NO_2 at different surface temperatures.

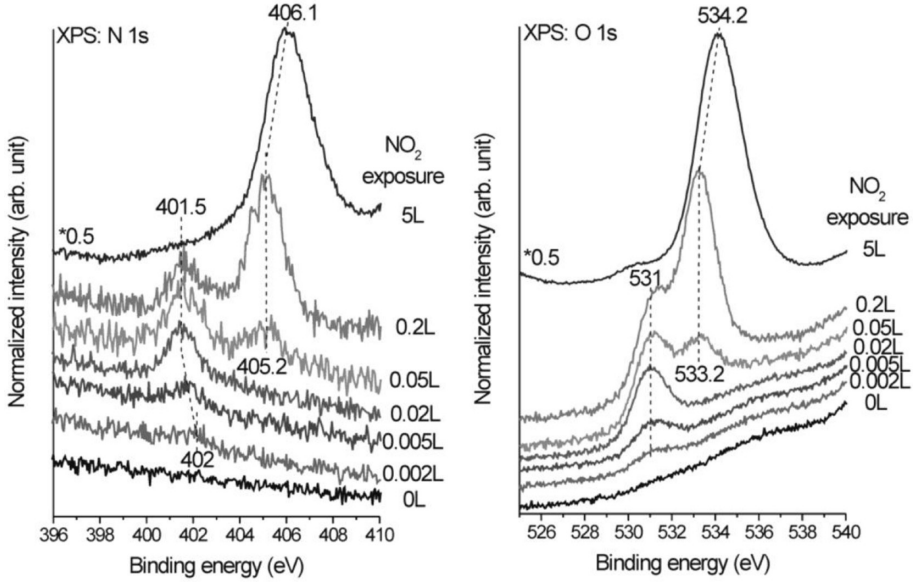

Figure 4. (Left) N 1s and (right) O 1s XPS spectra after Au(997) was exposed to different amounts of NO_2 at 130 K.

exposure is higher than 5 L (inset in Figure 2E) and at ~204 K when NO_2 exposure reaches 20 L (Figure 2B, Figure 2E, and inset in Figure 2D). Both imply the occurrence of novel surface reactions at large NO_2 exposures that will be discussed in the following part.

Figure 2F displays the desorption traces of O_2 after various exposures of NO_2 on clean Au(997) at 130 K. For NO_2 exposures below 0.1 L, no oxygen desorption can be observed in TDS spectra, suggesting that chemisorbed NO_2(a) does not decompose upon heating. When NO_2 exposure reaches 0.1 L, a symmetric O_2 desorption peak appears at ~560 K. With the increase of NO_2 exposure, the O_2 desorption feature grows and eventually develops into a main peak at ~538 K with two shoulders at ~520 and ~570 K. The recombination desorption of O(a) on Au single-crystal surfaces has been usually observed in the temperature range of 500−550 K.[43−51] Thus, above O_2 desorption peaks arise from the recombination desorption of O(a) on various sites of Au(997). Therefore, O(a) can be produced on Au(997) under UHV conditions by NO_2 exposure higher than 0.1 L at 130 K followed by heating. It is noteworthy that the physisorbed N_2O_4 multilayer begins to form on Au(997) at 0.1 L NO_2 exposure and grows with the increase of NO_2 exposure, implying the involvement of the N_2O_4 multilayer in O(a) formation. To prove this, we exposed 20 L NO_2 to the Au(997) surface at various temperatures whose TDS results are shown in Figure 3. It can be seen clearly that the O_2 desorption peak appears only after the NO_2 exposure at 130 K under which the temperature physisorbed N_2O_4 multilayer forms on Au(997). For 20 L NO_2 exposure at elevated temperatures in which the physisorbed N_2O_4 multilayer can not form, no O_2 desorption features could be detected. These results clearly demonstrate that O(a) adatoms produced on Au(997) in our case originate from a physisorbed N_2O_4 multilayer whose mechanism will be discussed in the following part. Therefore, on the basis of TDS results, NO_2 chemisorbs reversibly without decomposition on Au(997) at 130 K, agreeing with previous results that NO_2 chemisorbs molecularly even on the polycrystalline gold surface.[25] The (111) step sites of Au(997) bind with NO_2(a) more strongly than the (111) terrace sites of Au(997), agreeing with the general observation that low-coordinated Au atoms exhibit enhanced reactivity and the physisorbed N_2O_4 multilayer can undergo surface reactions to produce O(a) on Au(997). We have also done the TDS measurement following an exposure of 10 L NO_2 at 130 K with a −30 V bias on Au(997) whose results are similar to those without the bias, demonstrating that

dx.doi.org/10.1021/jp210028y | J. Phys. Chem. C 2012, 116, 3608−3617

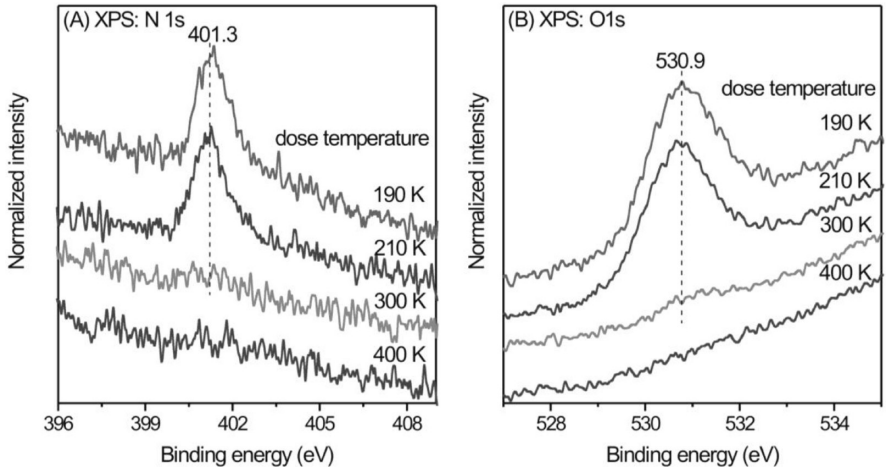

Figure 5. (A) N 1s and (B) O 1s XPS spectra after Au(997) was exposed to 20 L NO_2 at different surface temperatures.

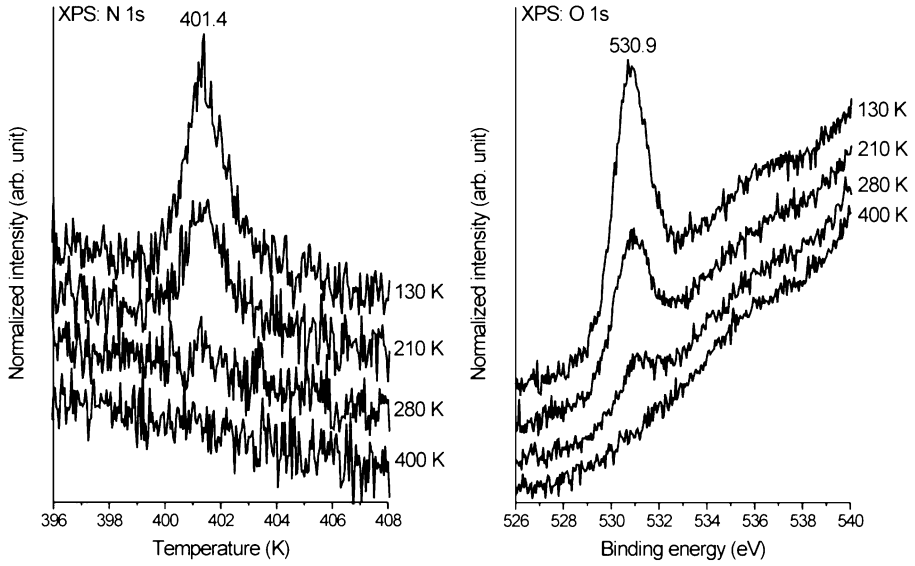

Figure 6. (A) N 1s and (B) O 1s XPS spectra after Au(997) was exposed to 0.02 L NO_2 at 130 K followed by annealing at various temperatures.

the formation of O(a) on Au(997) from the physisorbed N_2O_4 multilayer observed in TDS results is not likely to be induced by electrons from ionization filaments of the mass spectrometer.

Figure 4 shows N 1s and O 1s spectra after Au(997) was exposed to various amount of NO_2 at 130 K. Following 0.002 L NO_2 exposure, a single N 1s feature and a single O 1s feature appear at 402 and 531 eV, respectively. Both N 1s and O 1s features grow with the increase of NO_2 exposure up to 0.05 L and then saturate; meanwhile, the O 1s binding energy does not shift, but the N 1s binding energy shifts downward to 401.5 eV and then keeps unchanged. Following 0.05 L NO_2 exposure, a new N 1s peak appears at 405.2 eV and shifts to higher binding energy with the increasing of NO_2 exposure. Accordingly, a new O 1s peak also evolves with the binding energy at 533.2 eV, and its binding energy reaches 534.2 eV with a NO_2 exposure of 5.0 L. These values are in line with those of the N_2O_4 multilayer on other metal single-crystal surfaces,[8,17,52] and thus the corresponding species can be assigned to the N_2O_4 multilayer on Au(997). The molecular chemisorption of NO_2 on Au(111) and the polycrystalline Au surface have been previously reported by means of vibrational spectroscopy,[1,25] but no N 1s and O 1s binding energies have been reported for chemisorbed NO_2(a) on metal single-crystal surfaces. Previous results have shown that NO_2 is very reactive and does not molecularly chemisorb on metal single-crystal surfaces at 90 K or higher temperatures; instead, it dissociates into a NO(a) + O(a) mixed layer upon chemisorption which gives a N 1s binding energy between 400.9 and 402.1 eV.[6,17,52] It was recently reported that NO_2(a) chemisorbed on rutile TiO_2(110) gave a N 1s binging energy between 402.3 and 403.1 eV.[53] Although a single NO desorption peak arising from NO(a) on the (111) steps of Au(997) was observed at ~170 K in TDS after the saturating NO exposure at 130 K, XPS failed to detect any N 1s and O 1s signals likely due to the very low NO(a) coverage. Oxygen adatoms on Au surfaces with their O 1s feature between 529.2 and 530.1 eV[34,45] were not observed for NO_2 adsorption on Au(997) at 130 K, which could be taken as an indication for its molecular chemisorption. Moreover, no formation of O(a) was observed by XPS after exposure of 20 L NO_2 to Au(997) at elevated temperatures (Figure 5B), in consistence with the above TDS result that O(a) on Au(997) results from surface reactions of the physisorbed N_2O_4 multilayer; meanwhile, the resulting N 1s binding energy

dx.doi.org/10.1021/jp210028y | J. Phys. Chem. C 2012, 116, 3608–3617

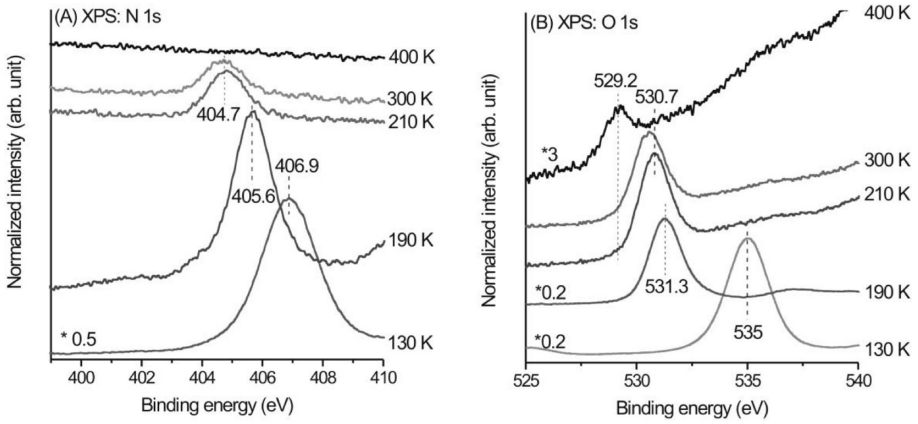

Figure 7. (A) N 1s and (B) O 1s XPS spectra after Au(997) was exposed to 20 L NO_2 at 130 K followed by annealing at various temperatures.

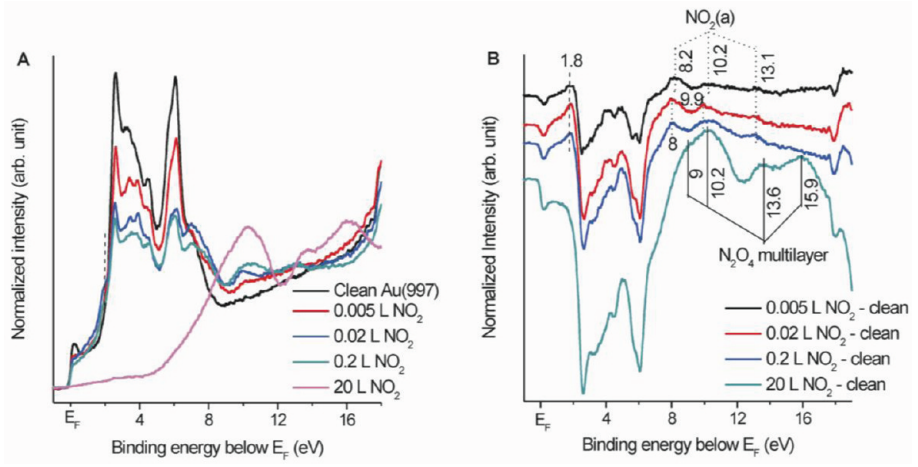

Figure 8. (A) He II UPS spectra and (B) UPS difference spectra after Au(997) was exposed to various amounts of NO_2 at 130 K.

does not shift (Figure 5A). These observations also imply that the interaction of NO_2 with Au(997) only forms molecularly chemisorbed NO_2(a). Thus, we assigned the surface species with a N 1s binding energy of 401.3−402 eV and an O 1s binding energy of ∼531 eV to chemisorbed NO_2(a) on Au(997).

Our TDS results suggest that O(a) on Au(997) is produced by surface reaction of the N_2O_4 multilayer, not by the decomposition of NO_2(a). Figures 6 and 7 display the evolution of N 1s and O 1s XPS spectra as a function of annealing temperature after Au(997) was exposed to 0.02 and 20 L NO_2 at 130 K, respectively. Chemisorbed NO_2(a) involving NO forms on the surface after an exposure of 0.02 L NO_2 at 130 K, giving the N 1s feature at 401.4 eV and the corresponding O 1s feature at 530.9 eV. Annealing the surface at 210 K leads to the attenuation of both N 1s and O 1s features, corresponding to the γ_2- and γ_3-NO desorption peaks; further increasing the annealing temperature to 280 K strongly weakens both N 1s and O 1s features, corresponding to the desorption of β-NO_2(a) species from the surface; and annealing at 400 K removes α-NO_2(a) species from the surface, and no signals could be detected by XPS. These results indicate that chemisorbed NO_2(a) on Au(997) molecularly desorbs from the surface upon heating.

After an exposure of 20 L NO_2 at 130 K, the N 1s and O 1s XPS spectra are dominated by the feature of the thick physisorbed N_2O_4 multilayer, respectively, giving its N 1s and O 1s peaks at 406.9 and 535.0 eV. After annealing at 190 K, the N_2O_4 multilayer desorbs from the surface, resulting in a significant reduction in the intensity of N 1s and O 1s peaks. Meanwhile, the N 1s binding energy shifts to 405.6 eV, and surprisingly, the O 1s binding energy shifts to 531.3 eV, indicating the formation of a new surface species. After further annealing at 210 K, both N 1s and O 1s peaks attenuate, corresponding to the desorption peak of NO_2 at ∼210 K that was only observed for very large NO_2 exposures (inset in Figure 2D); meanwhile, the N 1s and O 1s binding energies further shift downward to 404.7 and 530.7 eV, respectively, suggesting the formation of another new surface species. Both N 1s and O 1s peaks only slightly attenuate after annealing at 300 K, and the N 1s and O 1s binding energies do not shift much. After annealing at 400 K, the N 1s component completely disappears, while a weak but visible O 1s peak appears with the binding energy of 529.2 eV that can be reasonably assigned to O(a) on Au(997).[34,54] In combination with the above TDS results that NO and NO_2 desorption peaks were observed around 350 K (inset of Figure 2E) after large exposures of NO_2 at 130 K, it can be concluded that the new surface species characterized by its O 1s feature at 530.7 eV and its N 1s feature at 404.7 eV undergoes a decomposition reaction to produce O(a) on Au(997) and gaseous NO(g) and NO_2(g) between 300 and 400 K. By calculating the intensity ratio between the O 1s peak and Au 4f peak,[47] the O(a) coverage was estimated to be ∼0.1 ML. The formed O(a) on Au(997) then recombines to gaseous

dx.doi.org/10.1021/jp210028y | J. Phys. Chem. C 2012, 116, 3608−3617

O_2 prior to 600 K. These XPS results adequately support the TDS results that surface reactions of the physisorbed N_2O_4 multilayer on Au(997) upon heating lead to the formation of O(a).

We also employed UPS to study the interaction of NO_2 with Au(997). Figures 8A and 8B show the UPS spectra and the difference UPS spectra after Au(997) was exposed to various amounts of NO_2 at 130 K. Following an exposure of 0.005 L NO_2 that gives the α and β desorption peaks, four features appear at 1.8, 8.2, 10.2, and 13.1 eV below E_F in the UPS spectrum. The adsorption of NO_2 on metal single-crystal surfaces has seldom been studied with UPS, but NO(a) on single-crystal surfaces of Pt, Pd, Ru, and Rh has been characterized by UPS a lot and generally exhibits three features at 2−2.8, 8.8−9.8, and 13.6−14.6 eV below E_F corresponding to the 2π, $5\pi + 1\sigma$, and 4σ molecular orbitals of NO(a), respectively.[55−57] Bugyi et al.[58] reported the formation of KNO_2 upon NO adsorption on K-promoted Rh(111), in which three features at 4.0, 9.8, and 11.7 eV below E_F were observed in UPS and assigned to the $6a_1$, $1b_2$, and 1b + 5a molecular orbitals of NO_2^-. Although XPS failed to detect any N 1s and O 1s signals after the saturating NO exposure at 130 K, UPS observed a weak and diffuse peak at ∼11.8 eV below E_F. Therefore, the observed UPS features should result from the molecular chemisorption of NO_2(a) on Au(997). Comparing with gas-phase NO_2,[59] we assigned the peaks at 8.2, 10.2, and 13.1 eV below E_F, respectively, to the $4b_2 + 1a_2$, $5a_1 + 1b_1 + 3b_2$, and $4a_1$ molecular orbitals of NO_2(a) on Au(997) and the peak at 1.8 eV below E_F to the orbital splitting of the Au 5d band induced by the NO_2 chemisorption. The HOMO of NO_2(a) ($6a_1$ orbital) might be buried in the strong valence band of the substrate. When NO_2 exposure increases to 0.02 L, all features of NO_2(a) grow, in which two features at 8.2 and 10.2 eV below E_F slightly shift downward to 8 and 9.9 eV below E_F, respectively. With the further increase of NO_2 exposure, the N_2O_4 multilayer forms, giving four features at 9, 10.2, 13.6, and 15.9 eV below E_F that are comparable with those of gas-phase N_2O_4.[60]

Figure 9 shows the UPS difference spectra after Au(997) was exposed to 20 L NO_2 at 130 K followed by annealing at various temperatures. After the exposure of 20 L NO_2 at 130 K, the spectrum is dominated by the features of the N_2O_4 multilayer at 9, 10.2, 13.6, and 15.9 eV below E_F. Annealing the surface at 170 K desorbs the N_2O_4 multilayer, and thus their features disappear in the spectrum; however, other four features appear at 8.5, 10.3, 12.8, and 15.6 eV below E_F. These features grow after the annealing at 190 K but then disappear after the annealing at 210 K. Meanwhile, four features at 1.8, 6.8, 9.9, and 12.9 eV below E_F were observed in the spectrum. Two features at 1.8 and 6.8 eV below E_F can be assigned to the adsorbate-induced orbital splitting of the Au 5d band and the O 2p orbital of O(a) on Au(997), respectively. The appearance of O(a) on the surface could be related with the desorption traces of NO and NO_2 at ∼204 K (inset in Figure 2D). With the further increase of the annealing temperature up to 350 K, these two features slightly grow at the expense of the other two features at 9.9 and 12.9 eV below E_F. After annealing at 400 K, two features at 9.9 and 12.9 eV below E_F disappear. The O 2p orbital of O(a) on Au(997) at 6.8 eV below E_F grows, and the adsorbate-induced orbital-splitting feature of the Au 5d band shifts upward to 2.1 eV below E_F. These UPS results also adequately support the TDS results that surface reactions of the

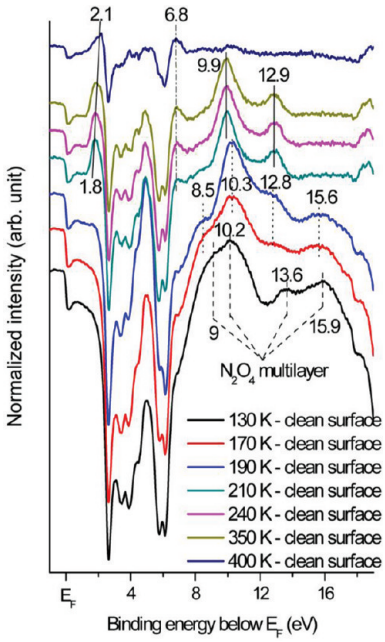

Figure 9. He II UPS difference spectra after Au(997) was exposed to 20 L NO_2 at 130 K followed by annealing at various temperatures.

physisorbed N_2O_4 multilayer on Au(997) upon heating lead to the formation of O(a).

The above experimental results of NO_2 adsorption on Au(997) at 130 K demonstrate two interesting observations. One is that low-coordinated Au atoms on the (111) steps of Au(997) do not dissociate chemisorbed NO_2(a), although they do bind NO_2(a) more strongly than Au atoms on the (111) terraces of Au(997). NO_2 was previously reported to adsorb molecularly on the Ar^+-sputtered Au(111) surface and polycrystalline Au surface,[25] but on other transitional metal surfaces including inert Ag(111), the decomposition of chemisorbed NO_2(a) is quite common.[20] Previous experimental results also demonstrate that low-coordinated Au atoms can exhibit enhanced reactivity toward CO and NO. CO can not adsorb on perfect Au(111), Au(100), and Au(311) surfaces at 120 K at CO pressures below 0.01 Torr[34] but can on Au(310), Au(321), Au(110)-(1 × 2), and Au(332) surfaces in the temperature range of 90−100 K.[33,35,36] NO can not adsorb on defect-free Au(111) even at a temperature of 90 K[1] but can adsorb on Au(111) with surface defects.[28] Furthermore, NO can even decompose into N_2O on Au(310) at temperature as low as 80 K.[37] We have also observed the chemisorption of CO and NO on the (111) steps of Au(997) at 130 K. These observations imply that the surface chemistry of NO_2 on Au surfaces is quite different from that on other transitional metal surfaces and also from surface chemistry of CO and NO on Au surfaces. The reaction of NO with O(a) on Au(111) has been studied both experimentally and theoretically,[28−30] in which NO was found to readily react with O(a) to form NO_2(a) that desorbs from the surface. We are also comparatively investigating the chemisorption of NO on clean and O(a)-covered Au(997) surfaces at 130 K. The preliminary TDS results are shown in Figure 10. Following saturating NO exposure on clean Au(997) at 130 K, the NO desorption peak was observed at ∼170 K. Following saturating NO exposure on the 0.06 ML O(a)-covered Au(997) surface at 130 K, the NO desorption peak was observed at ∼146 K with reduced

dx.doi.org/10.1021/jp210028y | J. Phys. Chem. C 2012, 116, 3608−3617

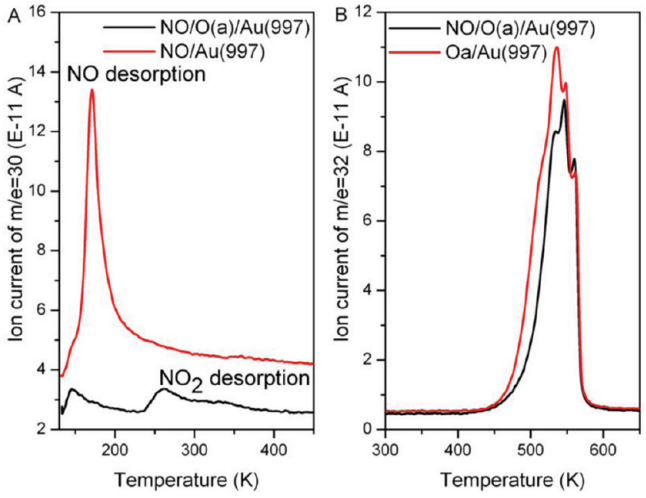

Figure 10. (A) TDS spectra of NO (m/e = 30) after saturating exposure of NO on clean Au(997) and 0.06 ML O(a)-covered Au(997) surfaces at 130 K. (B) TDS spectra of O_2 (m/e = 32) from ~0.06 ML O(a)-covered Au(997) surfaces without and with saturating exposure of NO at 130 K.

intensity, and another two desorption traces were observed at ~260 and ~335 K that should arise from the fragmentation of the NO_2 desorption trace; meanwhile, the intensity of the O_2 desorption peak also decreases. These preliminary results indicate that NO(a) can react with O(a) to form NO_2(a) on Au(997), agreeing with previous results on Au(111).[28−30] Therefore, NO_2(a) seems to be thermodynamically more stable than NO(a) + O(a) on the Au(997) surface, and upon heating, NO_2(a) on Au(997) prefers molecular desorption to thermal decomposition.

The other is that O(a) with coverage up to ~0.1 ML could be prepared as a result of surface reactions of the N_2O_4 multilayer by NO_2 exposure at 130 K followed by heating, although low-coordinated Au atoms do not dissociate NO_2(a). On the basis of the above TDS, XPS, and UPS results, during the course of heating up to 170 K, the N_2O_4 multilayer both desorbs from the surface and transforms into one surface intermediate characterized by the N 1s binding energy at 405.6 eV and O 1s binding energy at 531.3 eV and four valence features at 8.5, 10.3, 12.8, and 15.6 eV below E_F. This surface intermediate is thermally stable up to 190 K, but upon further heating, it both decomposes to NO(g), NO_2(g), and O(a) at ~204 K and transforms to another surface intermediate characterized by N 1s binding energy at 404.7 eV and O 1s binding energy at 530.7 eV and two valence features at 9.9 and 12.9 eV below E_F. This surface intermediate is thermally stable up to 350 K and then decomposes to NO(g), NO_2(g), and O(a). Estimated from the XPS spectra shown in Figure 7, the atomic O/N ratio of all surface species formed on Au(997) after the exposure of 20 L N_2O_4 at 130 K followed by annealing up to 300 K keeps ~2, implying that NO_3(a) is not likely to be the formed surface intermediates. On the basis of IRAS and TPD measurements, it has been proposed that the "free OH" of amorphous ice within the N_2O_4−H_2O coadsorbed layer formed on the Au(111) surface below 110 K could initiate the isomerization of O_2N−NO_2 to ONO−NO_2, and such nitrite−N_2O_4 might transform into nitrosonium nitrate ($NO^+NO_3^-$) at higher temperatures (200−260 K) which further decomposed above 275 K, releasing NO(g) and NO_2(g) and forming O(a) with coverage up to ~0.42 ML on Au(111).[26,27,61,62] However, by using IRAS, Sato et al. did not detect the presence of the above nitrite/nitrate intermediate in the temperature range 90−140 K for Au(111) covered by the H_2O−NO_2 coadsorption layer and proposed that the role of water in the H_2O−NO_2 coadsorption layer was to stabilize NO_2 by forming NO_2−H_2O adducts.[63] Givan and Loewenschuss have carried out a series of investigations of the solid N_2O_4 layer on inert substrates in which the order and composition of the N_2O_4 layer was found to depend largely on NO_2 deposition conditions.[64−67] The ordered N_2O_4 layer is very stable and desorbs reversibly from the surface; however, for the amorphous N_2O_4 layer, the nitrosonium nitrate ($NO^+NO_3^-$) can be formed during NO_2 deposition or heating to higher temperature with D′ isomers (O═$NONO_2$) as a probable precursor.[64,66]

To further elucidate if H_2O plays a role in the formation of O(a) on Au(997) under our experimental condition, a controlled experiment was conducted by exposing the Au(997) surface first to 0.2 L H_2O and then to 0.5 L NO_2 (0.2 L H_2O + 0.5 L NO_2) at 130 K, whose TDS result is shown in Figure 11. There do exist interactions between coadsorbed H_2O and NO_2, but the O_2 desorption spectrum after 0.2 L H_2O + 0.5 L NO_2 exposure is almost identical to that after 0.5 L NO_2 exposure. Therefore, the water-initiated isomerization of O_2N−NO_2 to ONO−NO_2 and further transformation of nitrite−N_2O_4 into nitrosonium nitrate ($NO^+NO_3^-$) are not likely to occur in our case.

Therefore, we propose that the N_2O_4 multilayer on the Au(997) surface under our experimental condition is with an amorphous phase. As schematically illustrated in Scheme 1,

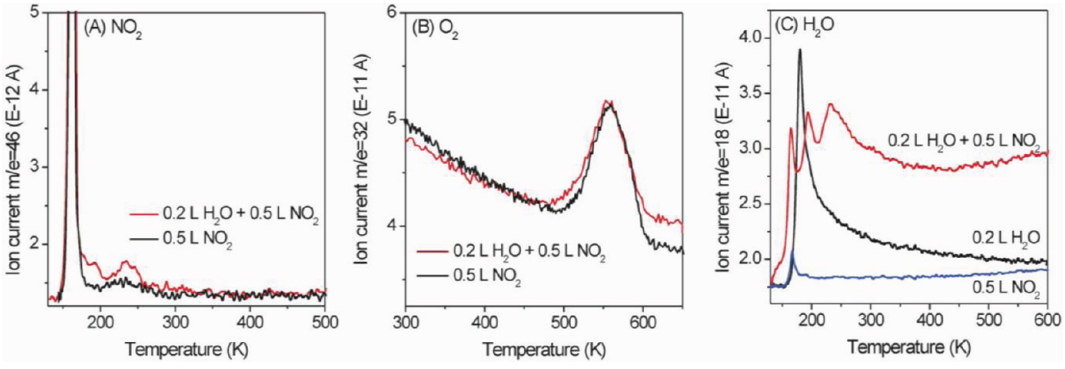

Figure 11. (A) NO_2 (m/e = 46), (B) O_2 (m/e = 32), and (C) H_2O (m/e = 18) TDS spectra after Au(997) was exposed to 0.5 L NO_2 and exposed to 0.2 L H_2O followed by 0.5 L NO_2 (0.2 L H_2O + 0.5 L NO_2) at 130 K.

dx.doi.org/10.1021/jp210028y | J. Phys. Chem. C 2012, 116, 3608−3617

Scheme 1. Schematic Illustration of Surface Reactions of the Amorphous Physisorbed N_2O_4 Multilayer to Form O(a) on Au(997)

$$O_2N-NO_2(a) \xrightarrow{<170K} ONO-NO_2(a)$$
$$ONO-NO_2(a) \xrightarrow{190-210K} NO_2(g)+NO(g)+O(a)+NO^+NO_3^-(a)$$
$$NO^+NO_3^-(a) \xrightarrow{350K} NO_2(g)+NO(g)+O(a)$$

upon heating, the amorphous N_2O_4 multilayer undergoes the following surface reactions to produce O(a) on the Au(997) surface: the amorphous physisorbed N_2O_4 multilayer (O_2N-NO_2) can isomerize to nitrite–N_2O_4 ($ONO-NO_2$) (<170 K), and at elevated temperatures (190–210 K), some nitrite–N_2O_4 decomposes to produce NO(g), NO_2(g), and O(a) on Au(997); other nitrite–N_2O_4 transforms into nitrosonium nitrate ($NO^+NO_3^-$), and nitrosonium nitrate further decomposes to produce NO(g), NO_2(g), and O(a) on the surface (~350 K). Therefore, nitrite–N_2O_4 ($ONO-NO_2$) is the surface intermediate with its N 1s binding energy at 405.6 eV and its O 1s binding energy at 531.3 eV and four valence features at 8.5, 10.3, 12.8, and 15.6 eV below E_F, and nitrosonium nitrate ($NO^+NO_3^-$) is the surface intermediate with its N 1s binding energy at 404.7 eV and its O 1s binding energy at 530.7 eV and two valence features at 9.9 and 12.9 eV below E_F.

Therefore, our results provide a practical method to prepare O(a) on inert Au surfaces under UHV conditions by exposing NO_2 at 130 K to form the N_2O_4 multilayer in the amorphous phase followed by heating. In the present study, the acquired maximum O(a) coverage can only reach ~0.1 ML, but we believe that higher O(a) coverage can be obtained by optimizing the experimental condition, for example, optimizing the heating rate to control the transformation processes from the amorphous N_2O_4 multilayer to nitrosonium nitrate. The reactivity of O(a) on the Au(997) surface is under investigation in our laboratory.

4. CONCLUSIONS

We have investigated the adsorption and surface reaction of NO_2 on a stepped Au(997) surface at 130 K by means of TDS, XPS, and UPS. The molecular adsorption and desorption of chemisorbed NO_2(a) on Au(997) are reversible, and low-coordinated Au atoms on the (111) step sites exhibit enhanced reactivity. NO_2(a) chemisorbed on the (111) step sites is thermally more stable than that chemisorbed on the (111) terrace sites. At large NO_2 exposures, the amorphous physisorbed N_2O_4 multilayer forms at 130 K. Subsequent heating causes the isomerization of the physisorbed N_2O_4 multilayer (O_2N-NO_2) to nitrite–N_2O_4 ($ONO-NO_2$) and the subsequent transformation of nitrite–N_2O_4 into nitrosonium nitrate ($NO^+NO_3^-$) that further decomposes into NO(g) and NO_2(g) at elevated temperatures, forming O(a) on the surface. The N 1s and O 1s binding energies of NO_2(a), $ONO-NO_2$(a), and $NO^+NO_3^-$(a) on Au(997) are located at 401.3–402 and ~531 eV, ~405.6 and ~531.3 eV, and ~404.7 and ~530.7 eV, respectively. These results broaden the fundamental understanding of the interaction between small molecules and Au surfaces.

AUTHOR INFORMATION

Corresponding Author

*Fax: + 86-551-3600437. E-mail: huangwx@ustc.edu.cn.

ACKNOWLEDGMENTS

This work is financially supported by National Natural Science Foundation of China (grant 20973161), the Ministry of Science and Technology of China (2010CB923302), the Fundamental Research Funds for the Central Universities, and the MPG-CAS partner group program.

REFERENCES

(1) Bartram, M. E.; Koel, B. E. *Surf. Sci.* **1989**, *213*, 137.
(2) Beckendorf, M.; et al. *J. Phys.: Condens. Matter* **1993**, *5*, 5471.
(3) Lu, X.; Xu, X.; Wang, N.; Zhang, Q. *J. Phys. Chem. A* **1999**, *103*, 10969.
(4) Sato, S.; Senga, T.; Kawasaki, M. *J. Phys. Chem. B* **1999**, *103*, 5063.
(5) Jirsak, T.; Kuhn, M.; Rodriguez, J. A. *Surf. Sci.* **2000**, *457*, 254.
(6) Jiang, Z.; Huang, W.; Tan, D.; Zhai, R.; Bao, X. *Surf. Sci.* **2006**, *600*, 4860.
(7) Price, G. L.; Sexton, B. A.; Baker, B. G. *Surf. Sci.* **1976**, *60*, 506.
(8) Fuggle, J. C.; Menzel, D. *Surf. Sci.* **1979**, *79*, 1.
(9) Dahlgren, D.; Hemminger, J. C. *Surf. Sci.* **1982**, *123*, L739.
(10) Schwalke, U.; Niehus, H.; Comsa, G. *Surf. Sci.* **1985**, *152–153*, 596.
(11) Schwalke, U.; Parmeter, J. E.; Weinberg, W. H. *Surf. Sci.* **1986**, *178*, 625.
(12) Bartram, M. E.; Windham, R. G.; Koel, B. E. *Surf. Sci.* **1987**, *184*, 57.
(13) Outka, D. A.; Madix, R. J.; Fisher, G. B.; Dimaggio, C. *Surf. Sci.* **1987**, *179*, 1.
(14) Geisler, H.; Odörfer, G.; Illing, G.; Jaeger, R.; Freund, H. J.; Watson, G.; Plummer, E. W.; Neuber, M.; Neumann, M. *Surf. Sci.* **1990**, *234*, 237.
(15) Brown, W. A.; Gardner, P.; King, D. A. *Surf. Sci.* **1995**, *330*, 41.
(16) Gibson, K. D.; Colonell, J. I.; Sibener, S. J. *Surf. Sci.* **1999**, *443*, 125.
(17) Jirsak, T.; Dvorak, J.; Rodriguez, J. A. *Surf. Sci.* **1999**, *436*, L683.
(18) Rodriguez, J. A.; Jirsak, T.; Liu, G.; Hrbek, J.; Dvorak, J.; Maiti, A. *J. Am. Chem. Soc.* **2001**, *123*, 9597.
(19) Huang, W.; Jiang, Z.; Jiao, J.; Tan, D.; Zhai, R.; Bao, X. *Surf. Sci.* **2002**, 506.
(20) Huang, W. X.; White, J. M. *Surf. Sci.* **2003**, *529*, 455.
(21) Yeo, B. S.; Chen, Z. H.; Sim, W. S. *Surf. Sci.* **2004**, *557*, 201.
(22) Alemozafar, A. R.; Madix, R. J. *Surf. Sci.* **2005**, *587*, 193.
(23) Deiner, L. J.; Kang, D. H.; Friend, C. M. *J. Phys. Chem. B* **2005**, *109*, 12826.
(24) Turner, M.; Vaughan, O. P. H; Lambert, R. M. *Chem. Commun.* **2008**, 2316.
(25) Wickham, D. T.; Banse, B. A.; Koel, B. E. *Catal. Lett.* **1990**, *6*, 163.
(26) Wang, J.; Koel, B. E. *J. Phys. Chem. A* **1998**, *102*, 8573.
(27) Carabineiro, S.; Nieuwenhuys, B. *Gold Bull.* **2009**, *42*, 288.
(28) McClure, S. M.; Kim, T. S.; Stiehl, J. D.; Tanaka, P. L.; Mullins, C. B. *J. Phys. Chem. B* **2004**, *108*, 17952.
(29) Torres, D.; González, S.; Neyman, K. M.; Illas, F. *Chem. Phys. Lett.* **2006**, *422*, 412.
(30) Zhang, W.; Li, Z.; Luo, Y.; Yang, J. *J. Chem. Phys.* **2008**, *129*, 134708.
(31) Haruta, M.; Kobayashi, T.; Sano, H.; Yamada, N. *Chem. Lett.* **1987**, *16*, 405.
(32) Lopez, N.; Janssens, T. V. W.; Clausen, B. S.; Xu, Y.; Mavrikakis, M.; Bligaard, T.; Nørskov, J. K. *J. Catal.* **2004**, *223*, 232.
(33) Weststrate, C. J.; Lundgren, E.; Andersen, J. N.; Rienks, E. D. L.; Gluhoi, A. C.; Bakker, J. W.; Groot, I. M. N.; Nieuwenhuys, B. E. *Surf. Sci.* **2009**, *603*, 2152.
(34) Nakamura, I.; Takahashi, A.; Fujitani, T. *Catal. Lett.* **2009**, *129*, 400.
(35) Ruggiero, C.; Hollins, P. *Surf. Sci.* **1997**, *377–379*, 583.
(36) Meier, D. C.; Bukhtiyarov, V.; Goodman, D. W. *J. Phys. Chem. B* **2003**, *107*, 12668.

(37) Vinod, C. P.; Hans, J. W. N.; Nieuwenhuys, B. E. *Appl. Catal., A* **2005**, *291*, 93.
(38) Fajín, J. L. C.; Cordeiro, M. N. D. S.; Gomes, J. R. B. *Appl. Catal., A* **2010**, *379*, 111.
(39) Xu, L.; Ma, Y.; Zhang, Y.; Jiang, Z.; Huang, W. *J. Am. Chem. Soc.* **2009**, *131*, 16366.
(40) Xu, L.; Ma, Y.; Zhang, Y.; Chen, B.; Wu, Z.; Jiang, Z.; Huang, W. *J. Phys. Chem. C* **2010**, *114*, 17023.
(41) Hahn, E.; Schief, H.; ouml; rg.; Marsico, V.; Fricke, A.; Kern, K. *Phys. Rev. Lett.* **1994**, *72*, 3378.
(42) Giesen, M.; Linke, U.; Ibach, H. *Surf. Sci.* **1997**, *389*, 264.
(43) Canning, N. D. S.; Outka, D.; Madix, R. J. *Surf. Sci.* **1984**, *141*, 240.
(44) Sault, A. G.; Madix, R. J.; Campbell, C. T. *Surf. Sci.* **1986**, *169*, 347.
(45) Saliba, N.; Parker, D. H.; Koel, B. E. *Surf. Sci.* **1998**, *410*, 270.
(46) Gottfried, J. M.; Schmidt, K. J.; Schroeder, S. L. M.; Christmann, K. *Surf. Sci.* **2003**, *525*, 184.
(47) Deng, X.; Friend, C. M. *J. Am. Chem. Soc.* **2005**, *127*, 17178.
(48) Deng, X. Y.; Min, B. K.; Guloy, A.; Friend, C. M. *J. Am. Chem. Soc.* **2005**, *127*, 9267.
(49) Gong, J. L.; Flaherty, D. W.; Ojifinni, R. A.; White, J. M.; Mullins, C. B. *J. Phys. Chem. C* **2008**, *112*, 5501.
(50) Baker, T. A.; Friend, C. M.; Kaxiras, E. *J. Phys. Chem. C* **2009**, *113*, 3232.
(51) Okazaki-Maeda, K.; Kohyama, M. *Chem. Phys. Lett.* **2010**, *492*, 266.
(52) Polzonetti, G.; Alnot, P.; Brundle, C. R. *Surf. Sci.* **1990**, *238*, 226.
(53) Haubrich, J.; Quiller, R. G.; Benz, L.; Liu, Z.; Friend, C. M. *Langmuir* **2010**, *26*, 2445.
(54) Lazaga Mark, A.; Wickham David, T.; Parker Deborah, H.; Kastanas George, N.; Koel Bruce, E. In *Catalytic Selective Oxidation*; American Chemical Society: Washington DC, 1993; Vol. *523*, p 90.
(55) Bonzel, H. P.; Fischer, T. E. *Surf. Sci.* **1975**, *51*, 213.
(56) Bertolo, M.; Jacobi, K. *Surf. Sci.* **1990**, *226*, 207.
(57) Sugai, S.; Watanabe, H.; Kioka, T.; Miki, H.; Kawasaki, K. *Surf. Sci.* **1991**, *259*, 109.
(58) Bugyi, L.; Kiss, J.; Révész, K.; Solymosi, F. *Surf. Sci.* **1990**, *233*, 1.
(59) Brundle, C. R.; Neumann, D.; Price, W. C.; Evans, D.; Potts, A. W.; Streets, D. G. *J. Chem. Phys.* **1970**, *53*, 705.
(60) Ames, D. L.; Turner, D. W. *Proc. R. Soc. London A* **1976**, *348*, 175.
(61) Wang, J.; Voss, M. R.; Busse, H.; Koel, B. E. *J. Phys. Chem. B* **1998**, *102*, 4693.
(62) Wang, J.; Koel, B. E. *Surf. Sci.* **1999**, *436*, 15.
(63) Sato, S.; Yamaguchi, D.; Nakagawa, K.; Inoue, Y.; Yabushita, A.; Kawasaki, M. *Langmuir* **2000**, *16*, 9533.
(64) Givan, A.; Loewenschuss, A. *J. Chem. Phys.* **1989**, *90*, 6135.
(65) Givan, A.; Loewenschuss, A. *J. Chem. Phys.* **1989**, *91*, 5126.
(66) Givan, A.; Loewenschuss, A. *J. Chem. Phys.* **1990**, *93*, 7592.
(67) Givan, A.; Loewenschuss, A. *J. Chem. Phys.* **1991**, *94*, 7562.